J Clust Sci (2017) 28:2005–2015
DOI 10.1007/s10876-017-1194-0

ORIGINAL PAPER

Two Novel Two-Dimensional Lanthanide (III) Coordination Polymers Constructed from Isonicotinic Acid and Iminodiacetic Acid: Synthesis, Structure, and Luminescence Properties

Wei Xu[1] · Chang-Juan Zhang[1] · Hua Wang[1] · Yi Wang[1]

Received: 26 January 2017 / Published online: 20 March 2017

Abstract Two novel two-dimensional Ln coordination polymers (CPs) $[Ln_3(\mu_3\text{-}OH)(IN)_3(HIDA)(IDA)_2]_n$ (Ln = Eu, **1**; Sm, **2**; HIN = isonicotinic acid, and H_2IDA = iminodiacetic acid) have been successfully synthesized under solvothermal conditions and characterized by IR, TG, and elemental analyses. The structures of **1** and **2** were determined by single-crystal X-ray structural analysis, which shows that Ln^{III} ions interconnect through HIN and H_2IDA molecules to generate a 1D chain, and the adjacent chains are joined together by the same form to form the 2D zonary plane of **1** and **2**. Meanwhile, We also studied luminescence properties of **1** and **2**. The luminescence lifetime and quantum yield of **1** are 1.32 ms and 25.30%, which are significantly longer and higher than the values obtained for reported Eu^{3+} coordination polymers in the solid state at room temperature.

Electronic supplementary material The online version of this article (doi:10.1007/s10876-017-1194-0) contains supplementary material, which is available to authorized users.

✉ Wei Xu
tracy_xu1984@yeah.net

Chang-Juan Zhang
353855325@qq.com

Hua Wang
29871640@qq.com

Yi Wang
626651828@qq.com

[1] School of Environmental and Pharmaceutical Engineering, Taizhou Institute of Science and Technology, NUST, Taizhou 225300, China

Graphical Abstract

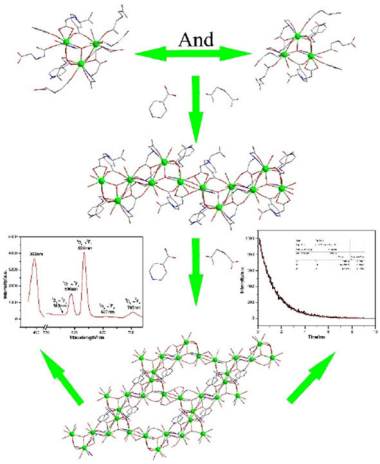

Keywords Ln MOFs · Luminescence lifetime and quantum yield · H_2IDA · HIN

Introduction

As a new class of porous materials, metal–organic frameworks(MOFs), a class of crystalline hybrid inorganic–organic materials formed by the connection of metal centers or clusters and organic linkers, have attracted tremendous attention for their wide applications in the areas of gas storage/separation [1–3], catalysis [4–6], magnetism [7, 8], drug delivery [9], sensors [10, 11], etc. Thus, a large number of MOFs have been designed and developed from various metal ions and organic ligands [12, 13]. Therefore, the luminescent MOFs have drawn special attention owing to their various applications in biomedical areas, optical displays, energy-harvesting device amplification, and fluorescent probes [14, 15]. The most interesting examples of luminescent MOFs are lanthanide (III) (Ln^{III}) complexes because of their high quantum yield, large Stokes shift, and long emission lifetimes [16, 17].

To obtain lanthanide (III) (Ln^{III}) complexes, a binding site and a powerful luminophore is required [18, 19]. Therefore, it is important to select appropriate ligands. On one hand, when constructing Ln-MOFs, organic ligands can not only serve as connective building blocks for the structure but can also function as antennae for the lanthanide ions [20–22]. In view of the previous work [23–26], carboxylate ligands are a good choice because Ln^{3+} ions are hard acceptors, making coordination with the hard carboxylate oxygen atoms more favorable, according to the "hard-soft acid-base" concept. Moreover, aromatic carboxylic groups are good luminescent chromophores, resulting in the intense luminescence of lanthanide. For example, isonicotinic acid (HIN)/iminodiacetic acid (H_2IDA), containing carboxylate groups, have been used previously in lanthanide (III) (Ln^{III}) complexes [27, 28].

Alternatively, amino nitrogen of H_2IDA can also be considered as binding sites and be immobilized in luminescent MOFs.

For this purpose, we choose HIN and H_2IDA reacting with lanthanide oxides in ethanol solution by self-assembly approach and obtained two trinuclear $\left(Ln_3^{III}\right)$ complexes, $[Ln_3\ (\mu_3\text{-OH})\ (IN)_3\ (HIDA)\ (IDA)_2]_n$ (Ln = Eu, **1**; Sm, **2**). Meanwhile, We also studied luminescence properties of **1** and **2**. The luminescence lifetime and quantum yield of **1** are 1.32 ms and 25.30%, which are significantly longer and higher than the values obtained for reported Eu^{3+} coordination polymers in the solid state at room temperature.

Experimental Section

Materials and Methods

All chemicals purchased were of reagent grade and were used without further purification. Powder X-ray diffraction (PXRD) were obtained on a Bruker D8X diffractometer equipped with monochromatized Cu Kα (λ = 1.5418 Å) radiation at room temperature. Data were collected in the range of 5°–50°, and the experimental XRD patterns are in agreement with the patterns simulated on the basis of the single-crystal structures. IR spectra were recorded on a Nicolet Impact 410 Fourier transform infrared spectrometer using KBr pellets in the 4000–500 cm^{-1} region. TG measurement was carried out on a Diamond thermogravimetric analyser in a flowing N_2 atmosphere from 25 to 1000 °C with a heating rate of 10 °C min^{-1}. The solid-state emission/excitation spectra were measured on an FP-6500 spectrofluorimeter equipped with a 450 W xenon lamp as the excitation source. Single-crystal structure determination was performed on a Bruker APEX2 CCD diffractometer at 296 K and a sealed tube X-ray source (Mo Kα radiation, λ = 0.71073 Å) operating at 50 kV and 30 mA.

Synthesis of $[Eu_3\ (\mu_3\text{-OH})\ (IN)_3\ (HIDA)\ (IDA)_2]_n$ ***(1)***

A mixture of Eu_2O_3(0.1760 g, 0.5 mmol), HIN (0.1231 g, 1.0 mmol), H_2 IDA(0.1331 g, 1.0 mmol), ethanol (8 mL) was stirred for 12 h in the air until all reagents dissolve, then this solution was sealed in a 25 mL Teflon-lined autoclave and kept at 170 °C for seven days. Cooled to room temperature under natural cooling. Yellow block crystal were obtained (0.1555 g, yield of 37.88% based on Eu), which were washed with ethanol and dried at room temperature for 24 h. IR (cm^{-1}): 1583 (vs), 1419 (s), 1312 (w), 1260 (w), 1120 (w), 1020 (w), 1005 (w), 646 (w). Elemental analysis calc: C, 29.23, H, 2.19, N, 6.82%; found: C, 29.35, H, 2.26, N, 6.78%.

Synthesis of $[Sm_3\ (\mu_3\text{-OH})\ (IN)_3\ (HIDA)\ (IDA)_2]_n$ ***(2)***

Complex **2** as yellow block single crystals was prepared (0.1505 g, yield of 36.70% based on Sm) according to the same procedure as **1**, except with Eu_2O_3 instead of

Sm_2O_3 (0.1744 g, 0.5 mmol). IR (cm^{-1}): 1607 (vs), 1417 (s), 1323 (w), 1255 (w), 1125 (w), 1007 (w), 917 (w), 611 (w). Elemental analysis calc: C, 29.35, H, 2.20, N, 6.85%; found: C, 29.41, H, 2.29, N, 6.74%.

X-ray Crystallography

Data for the compounds of **1** and **2** were collected by using a Bruker Apex 2 CCD single-crystal diffractometer with Mo Kα radiation ($\lambda = 0.71073$Å) at 296(2) using ω-2θ scan method. The single crystals of all compounds **1** and **2** were chosen and held on a thin glass fiber by epoxy glue in air for data collection. The SHELX software package (Bruker) was used to solve and refine the structures. Absorption corrections were applied empirically using the SADABS program. All the non-hydrogen atoms were refined anisotropically. The hydrogen atoms of organic molecule were placed in calculated positions, assigned isotropic thermal parameters, and allowed to ride on their parent atoms, while the H atoms of water and disordered organic molecules were not located. A total of two structures were solved by direct methods and refined on F^2 by full-matrix least-squares methods using the SHELX-2014/7 crystallographic software package. All non-H atoms were refined anisotropically. Further details of the X-ray structural analyses for compounds **1** and **2** are given in Table 1. The selected bond lengths for **1** and **2** are listed in Tables S1–S2, respectively. Crystallographic data for the structure reported in this paper has been deposited in the Cambridge Crystallographic Data Center with CCDC Numbers 1527504–1527505 for **1** and **2**.

Results and Discussion

Synthesis

Solvothermal synthesis has recently been demonstrated to be a powerful method in the synthesis of solid-state rare-earth clusters. During a specific solvothermal synthesis, many factors can affect the nucleation and crystal growth of the final products, such as the type of initial reactants, starting concentrations of the reactants, pH values, solvents, reaction temperature and reaction time. In our case, the temperature has great influence on the yields of **1** and **2**. We tried to change the reaction temperature to 80–170 °C, and the yields are the highest when the reaction temperature is 170 °C. Although ethanol is not included in the final products, but we cannot obtain the above 2 compounds without ethanol. Therefore, ethanol can be used as structure directing agent. The above compounds could be easily obtained under solvothermal synthesis and have good reproducibility.

Crystal Structures

Single-crystal X-ray diffraction analyses revealed that compounds **1**–**2** are isostructural and their crystal system, space group, unit cell dimensions, related bond distances, and bond angles are only slightly different. Therefore, only the

Table 1 Crystal data and structure refinements for **1** and **2**

Compound	**1**	**2**
Formula	$C_{30}H_{27}O_{19}N_6Eu_3$	$C_{30}H_{27}O_{19}N_6Sm_3$
Formula weight	1231.45	1226.62
T (K)	296 (2)	296 (2)
Wavelength (Å)	0.71073	0.71073
Crystal system	Triclinic	Triclinic
Space group	P−1	P−1
a (Å)	12.088 (7)	12.080 (7)
b (Å)	13.502 (7)	13.505 (8)
c (Å)	14.231 (8)	14.176 (9)
α (°)	61.831 (6)	62.027 (7)
β (°)	65.768 (6)	66.000 (7)
γ (°)	76.237 (7)	76.386 (7)
V ($Å^3$)	1864.4 (17)	1863 (2)
Z	2	2
D_c (g/m^3)	2.194	2.187
Absorption coefficient (mm^{-1})	5.074	4.755
Crystal size (mm)	0.23 × 0.22 × 0.18	0.23 × 0.22 × 0.18
F (000)	1180	1174
θ range (°)	1.713–24.998	1.710–24.998
Limiting indices	$-14 \le h \le 13$	$-14 \le h \le 13$
	$-16 \le k \le 16$	$-16 \le k \le 15$
	$-16 \le l \le 16$	$-16 \le l \le 16$
Reflections collected	13,282	13,206
Independent reflections	6476 [R(int) = 0.0401]	6446 [R(int) = 0.0489]
Completeness	98.6%	98.4%
Data/restraints/parameters	6476/12/523	6446/42/513
GOF	0.993	0.912
Final R indices [I > 2sigma(I)]	R1 = 0.0360, wR2 = 0.0720	R1 = 0.0409, wR2 = 0.0941
R indices (all data)	R1 = 0.0569, wR2 = 0.0778	R1 = 0.0546, wR2 = 0.1012

structure of **1** will be discussed in detail. Compound **1** crystallizes in the triclinic space group $P-1$. The structure unit of **1** contains three crystallographically independent Eu atoms, one μ_3-OH^-, three IN^-, one $HIDA^-$ and two IDA^{2-} (Fig. 1). The Eu(III) center adopts a NO_8 donor set completed by one N donor coming from the H_2IDA molecule and eight oxygen atoms belonging to one μ_3-OH^-, one HIN molecules, and four different H_2IDA molecules (Fig. S8). The Eu–O distances are from 2.391(5) to 2.511(5) Å and the O–Eu–O bond angles range from 68.27(18) ° to 147.57(16) °. The values fall into the reported normal range [29]. Scheme 1 shows the coordination modes of H_2IDA and HIN ligands: the former adopts the 4.22101 and 5.22111 (using Harris notation [30]) coordination modes to

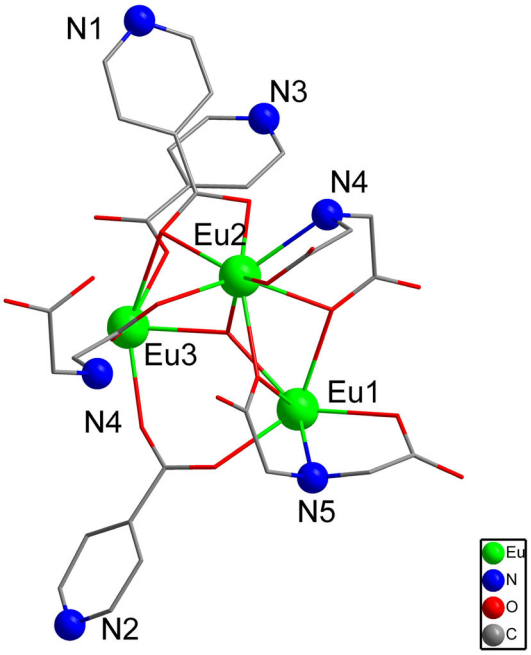

Fig. 1 View of the asymmetric unit of compound **1** (all H atoms omitted for clarity)

coordinate with metal atoms (I: coordinating with four Eu atoms, II: coordinating with five Eu atoms), and the latter adopts the 2.11 and 2.21 coordination modes to coordinate two Eu atoms.

In order to understand the structure of compound **1** clearly, we can view [Eu_3] as a unit. According to different arrangements in space, this unit can be divided into unit A (Fig. 2a) and unit B (Fig. 2b). Then, along the c-axis, 1D chain (Fig. 2c) is formed by units A connected to unit B through HIN and H_2IDA molecules. The adjacent chains are joined together by the same form to form the 2D zonary plane of **1** (Fig. 2d).

Powder X-ray Diffraction

The measured and simulated powder X-ray diffraction (PXRD) patterns of **1** and **2** are shown in Fig. S1-S2. The measured XRD patterns are in agreement with the calculated patterns, which indicate the phase purity of compounds **1** and **2**. The difference in reflection intensities during collection of the experimental XRD data are probably due to the preferred orientation effect of the powder.

IR Spectra

The IR spectra of **1** and **2** are presented in Fig. S3–S4. Because **1** and **2** are isomorphic, and only the IR spectra of **1** is discussed in detail. Bands originating from carboxylate anion vibrations are: (1) asymmetric stretch ν_{asym} (COO^-) located

Scheme 1 The crystallographically established coordination modes of H_2IDA and HIN in complex **1** and the Harris notation [30] which describes these modes

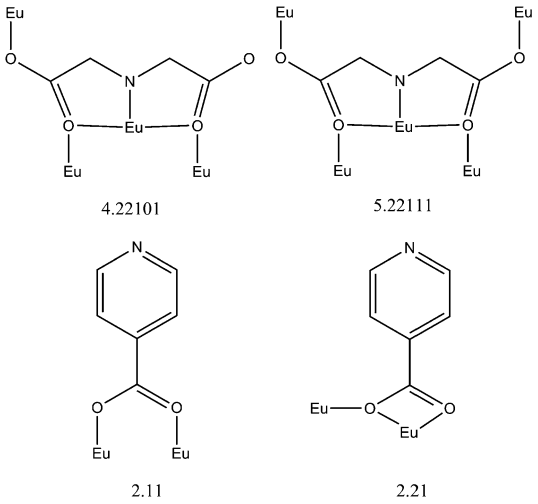

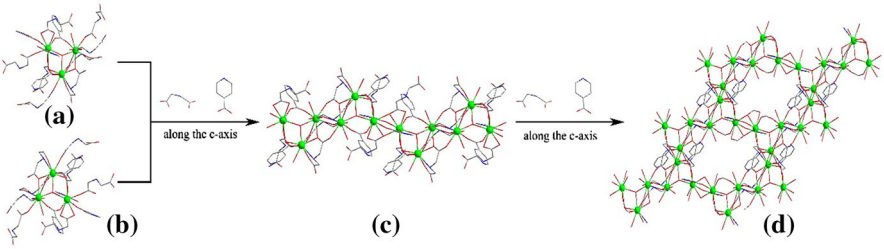

Fig. 2 **a** [Eu_3] unit A in **1**. **b** [Eu_3] unit B in **1**. **c** 1D chain formed by unit A and unit B along the c-axis. **d** View of 2D zonary structure of **1** formed along the c-axis

at 1596 cm^{-1}; (2) symmetric stretch ν_{sym} (COO^-) at 1397 cm^{-1}. The peaks in the range of 610–750 cm^{-1} for **1** correspond to the ν (Eu–O) vibrations. The features are in agreement with the reported compounds [31].

Thermal Analysis

The thermogravimetric (TG) analysis experiments were performed under N_2 atmosphere in the range of 25–1000 °C. Thermal analysis shows that the **1** and **2** are analogous in Fig. S5–S6. Take **1** as an example. As shown in Fig. S5, there is no obvious weight loss from room temperature to about 350 °C. Complex **1** exhibits an apparent weight loss of 54.50% from 350 to 735 °C, matching with the calculated value of releasing HIN and H_2IDA ligands molecules (calcd 55.81%). Further heating above 735 °C gives rise to the collapse of the framework. The final residual weight was 42.51% corresponding to the Eu_2O_3 (calc. 42.88%).

Luminescence Property

The luminescent behavior of Ln-based compounds has attracted increasing interest due to the high color purity and technological applications in light-emitting diodes, lasers, plasma displays, and sensory probes and optical amplifiers, etc. [32–34]. Because the good shielding of the 4*f* electrons by the outer 5*s* and 5*p* electrons leads to well-defined absorption and emission bands [35], Ln ions still keep their atomic properties upon complex formation. As a result, the luminescence properties of **1** and **2** in the solid-state have been measured at room temperature. As shown in Fig. 3, under 396 nm excitation wavelength solid emission spectrum of compound **1** demonstrates a characteristic transition of Eu^{3+}: $^5D_0 \rightarrow {}^7F_0$ (580 nm), $^5D_0 \rightarrow {}^7F_1$ (596 nm), $^5D_0 \rightarrow {}^7F_2$ (620 nm), $^5D_0 \rightarrow {}^7F_3$ (657 nm), and $^5D_0 \rightarrow {}^7F_4$ (705 nm). The existence of $^5D_0 \rightarrow {}^7F_0$ (580 nm) symmetry-forbidden transition emission spectrum illustrates Eu^{3+} is in the presence of a non-centrosymmetric coordination environment. As we know, the magnetic dipole transition $^5D_0 \rightarrow {}^7F_1$ is insensitive and hardly varies with the coordination environment, whereas the electric dipole transition $^5D_0 \rightarrow {}^7F_2$ is a hypersensitive transition, whose intensity is very sensitive and apt to be influenced by the host environment [36, 37]. From the figure, we can clearly see that $^5D_0 \rightarrow {}^7F_2$ (the electric dipole transition emission peak) is significantly stronger than the $^5D_0 \rightarrow {}^7F_1$, which also indicates that Eu^{3+} has the lower symmetric coordination environment. The dynamics of the Eu^{3+} PL (photoluminescence) was measured at room temperature (Fig. 4). The luminescence decay was successfully fitted by ways of a single exponential law (square correlation factor $R^2 > 0.99$). The luminescence lifetime and quantum yield of **1** are 1.32 ms and 25.30%, which are significantly longer and higher than the values obtained for reported Eu^{3+} coordination polymers in the solid state at room temperature [38, 39]. The major reason for which may have two factors: (a) there

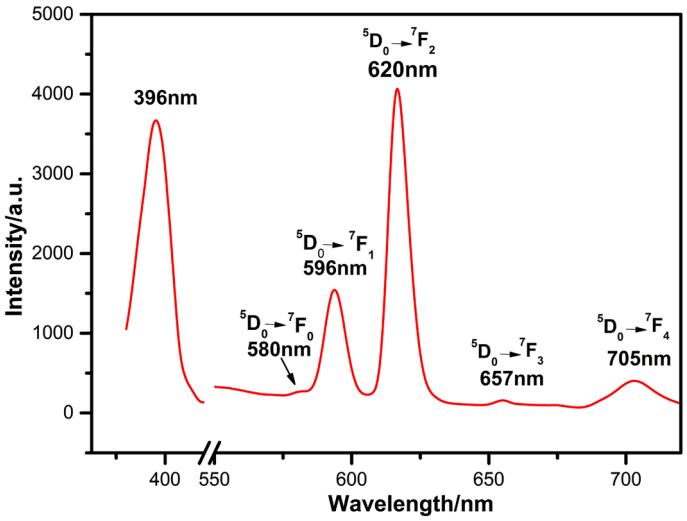

Fig. 3 Solid-state emission spectrum of **1** at room temperature

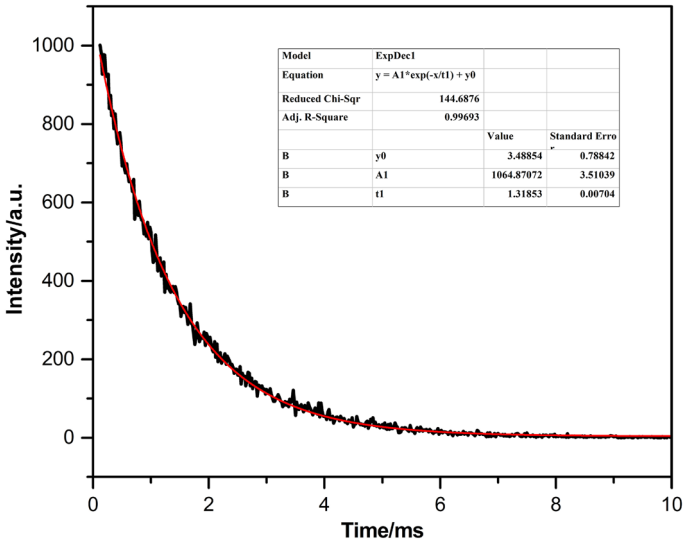

Fig. 4 Decay curve of Eu^{3+} in **1**

are not coordination waters and OH groups in **1**, which cannot quench emission and shorten luminescence lifetime through non-radiative relaxation processes [40]; (b) in **1**, each Eu^{III} cation is coordinated by a HIN ligand and four H_2IDA ligands that more effectively sensitize the Eu^{III} emission.

As shown in Fig. 5, complex **2** displays the characteristic emissions of the Sm(III) ion at 565, 596, 646, and 709 nm, which correspond to the $^4G_{5/2} \rightarrow {}^6H_J$ (J = 5/2, 7/2, 9/2, 11/2) transitions. The dynamics of the Sm^{3+} PL was measured at

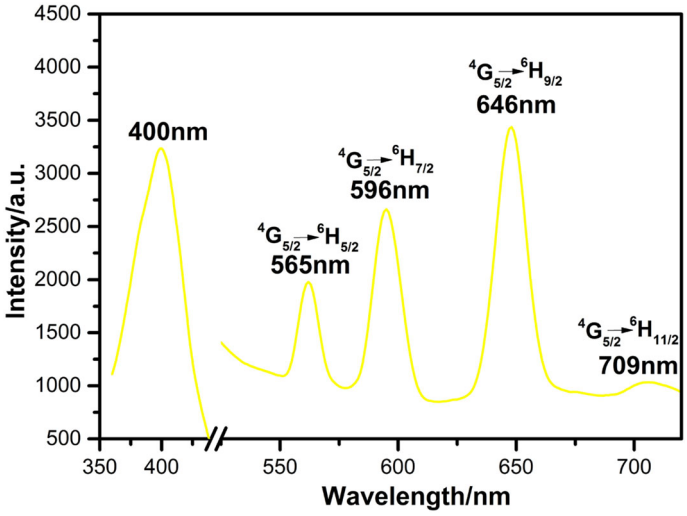

Fig. 5 Solid-state emission spectrum of **2** at room temperature

room temperature (Fig. S7). The luminescence decay was successfully fitted by ways of a single exponential law (square correlation factor $R^2 > 0.99$). From the decay curve of $^4G_{5/2} \rightarrow {}^6H_{9/2}$ from Sm^{3+} in **2** under 400 nm excitation, the decay lifetime was determined to be 35.5 μs. The quantum yield of **2** is 1.20%, which is higher than the values obtained for reported Sm^{3+} coordination polymers in the solid state at room temperature [41].

Conclusions

In summary, two novel two-dimensional lanthanide (III) coordination polymers constructed from isonicotinic acid and iminodiacetic acid have been synthesized. Of particular interest, **1** and **2** show good luminescence properties. Further systematic studies for the design and synthesis of such crystalline materials based on the HIN and H_2IDA ligands are currently under way.

References

1. K. Liu, B. Y. Li, Y. Li, X. Li, F. Yang, G. Zing, Y. Peng, Z. J. Zhang, G. H. Li, Z. Shi, S. H. Feng, and D. T. Song (2014). *Chem. Commun.* **50**, 5031.
2. Y. Liu, S. F. Wu, G. Wang, G. P. Yu, J. G. Guan, C. Y. Pan, and Z. G. Wang (2014). *J. Mater. Chem. A.* **2**, 7795.
3. H. M. Yin, J. Q. Wang, Z. Xie, J. H. Yang, J. Bai, J. M. Lu, Y. Zhang, D. H. Yin, and J. Y. S. Lin (2014). *Chem. Commun.* **50**, 3699.
4. O. Kozachuk, I. Luz, F. X. L. Xamena, H. Noei, M. Kauer, H. B. Albada, E. D. Bloch, B. Marler, Y. M. Wang, M. Muhler, and R. A. Fischer (2014). *Angew. Chem. Int. Ed.* **53**, 1.
5. K. Manna, T. Zhang, and W. B. Lin (2014). *J. Am. Chem. Soc.* **136**, 6566.
6. M. Yoon, R. Srirambalaji, and K. Kim (2011). *Chem. Rev.* **112**, 1196.
7. Z. Q. Xu, W. Meng, H. J. Li, H. W. Hou, and Y. T. Fan (2014). *Inorg. Chem.* **53**, 3260.
8. P. Dechambenoit and J. R. Long (2011). *Chem. Soc. Rev.* **40**, 3249.
9. S. Rojas, E. Quartapelle Procopio, F. J. Carmona, M. A. Romero, J. A. R. Navarro, and E. Barea (2014). *J. Mater. Chem. B.* **2**, 2473.
10. D. X. Ma, B. Y. Li, X. J. Zhou, Q. Zhou, K. Liu, G. Zeng, G. H. Li, Z. Shi, and S. H. Feng (2013). *Chem. Commun.* **49**, 8964.
11. M. Zhang, G. Feng, Z. G. Song, Y. P. Zhou, H. Y. Chao, D. Q. Yuan, T. T. Y. Tan, Z. G. Guo, Z. G. Hu, B. Z. Tang, B. Liu, and D. Zhao (2014). *J. Am. Chem. Soc.* **136**, 7241.
12. M. Li, D. Li, M. O'Keeffe, and O. M. Yaghi (2014). *Chem. Rev.* **114**, 1343.
13. S. L. James (2003). *Chem. Soc. Rev.* **32**, 276.
14. D. Sarma, M. Prabu, S. Biju, M. L. P. Reddy, and S. Natarajan (2010). *Eur. J. Inorg. Chem.* **24**, 3813.
15. J. Rocha, L. D. Carlos, F. A. A. Paz, and D. Ananias (2011). *Chem. Soc. Rev.* **40**, 926.
16. L. D. Carlos, R. A. S. Ferreira, V. D. Bermudez, and S. J. L. Ribeiro (2009). *Adv. Mater.* **21**, 509.
17. M. D. Allendorf, C. A. Bauer, R. K. Bhakta, and R. J. T. Houk (2009). *Chem. Soc. Rev.* **38**, 1330.
18. S. Liu, Z. Xiang, Z. Hu, X. Zheng, and D. Cao (2011). *J. Mater. Chem.* **21**, 66493.
19. Y. Q. Xiao, Y. J. Cui, Q. Zheng, S. C. Xiang, G. D. Qian, and B. L. Chen (2010). *Chem. Commun.* **46**, 5503.
20. H. B. Zhang, L. J. Zhou, J. Wei, Z. H. Li, P. Lin, and S. W. Du (2012). *J. Mater. Chem.* **22**, 21210.
21. H. H. Li, W. Shi, N. Xu, Z. J. Zhang, Z. Niu, T. Han, and P. Cheng (2012). *Cryst. Growth Des.* **12**, 2602.
22. H. Wang, S. J. Liu, D. Tian, J. M. Jia, and T. L. Hu (2012). *Cryst. Growth Des.* **12**, 3263.
23. J. M. Zhou, W. Shi, N. Xu, and P. Cheng (2013). *Inorg. Chem.* **52**, 8082.

24. B. Zhao, X. Y. Chen, Z. Chen, W. Shi, P. Cheng, S. P. Yan, and D. Z. Liao (2009). *Chem. Commun.* **21**, 3113.
25. M. L. P. Reddy and S. Sivakumar (2013). *Dalton Trans.* **42**, 2663.
26. A. R. Ramya, D. Sharma, S. Natarajan, and M. L. P. Reddy (2012). *Inorg. Chem.* **51**, 8818.
27. X. J. Gu and D. F. Xue (2007). *Inorg. Chem.* **46**, 5349.
28. J. B. Peng, Q. C. Zhang, X. J. Kong, Y. Z. Zheng, Y. P. Ren, L. S. Long, R. B. Huang, L. S. Zheng, and Z. Zheng (2012). *J. Am. Chem. Soc.* **134**, 3314.
29. J. W. Zhao, H. L. Li, Y. Z. Li, C. Y. Li, Z. L. Wang, and L. J. Chen (2014). *Cryst. Growth Des.* **14**, 5495.
30. R. A. Coxall, S. G. Harris, D. K. Henderson, S. Parsons, P. A. Tasker, and R. E. P. Winpenny (2000). *J. Chem. Soc. Dalton Trans.* **14**, 2349.
31. L. J. Chen, F. Zhang, X. Ma, J. Luo, and J. W. Zhao (2015). *Dalton Trans.* **44**, 12598.
32. F. S. Richardson (1982). *Chem. Rev.* **82**, 541.
33. S. J. A. Pope, B. J. Coe, S. Faulkner, E. V. Bichenkova, X. Yu, and K. T. Douglas (2004). *J. Am. Chem. Soc.* **126**, 9490.
34. J. C. G. Buünzli and C. Piguet (2005). *Chem. Soc. Rev.* **34**, 1048.
35. G. J. Sopasis, M. Orfanoudaki, P. Zarmpas, A. Philippidis, M. Siczek, T. Lis, J. R. O'Brien, and C. J. Milios (2012). *Inorg. Chem.* **51**, 1170.
36. G. R. Choppin and D. R. Peterman (1998). *Coord. Chem. Rev.* **174**, 283.
37. P. T. Ma, R. Wan, Y. N. Si, F. Hu, Y. Y. Wang, J. Y. Niu, and J. P. Wang (2015). *Dalton Trans.* **44**, 11514.
38. X. F. Li, Y. B. Huang, and R. Cao (2012). *Dalton Trans.* **41**, 6195.
39. X. Ma, X. Li, Y. E. Cha, and L. P. Jin (2012). *Cryst. Growth Des.* **12**, 5227.
40. D. T. Lill, A. Bettencourt-Dias, and C. L. Cahill (2007). *Inorg. Chem.* **46**, 3960.
41. W. S. Lo, J. H. Zhang, W. T. Wong, and G. L. Law (2015). *Inorg. Chem.* **54**, 3725.